



ANALYSIS OF CORNER BEAM-COLUMN JUNCTION WITH INCLUSION OF THE EFFECT OF CONSTRUCTION JOINTS

Prof. Dr. Husain M. Husain
University of Tikrit

Dina M. Hamza
M.Sc. Graduate
University of Baghdad

ABSTRACT

This paper describes a comparison between beam-column junctions with and without construction joint, also, a parametric study deals with construction joint is presented by taking various conditions of the junction. These include the various positions of the construction joint, the axial load on the column, strength of concrete in the second cast and the amount of dowels crossing the joint. By developing a computer program which was originally written by Dr. Ihsan Al-Shaarba (1990), (P3DNFEA, program of three dimensional nonlinear finite element analysis), to consider the effect of construction joint depending on the fact that the shear force can be transmitted across the shear plane either by interlocking of the aggregate particles protruding from each face or by dowel action of the reinforcement crossing the cracks by using Fronteddu's and Millard's models, respectively. It is concluded that the construction joints existed in the beam-column junctions result in a significant reduction in the in-plane shear stiffness and it would affect only on the rotation and shear strains of the joint.

الخلاصة

هذا البحث تضمن مقارنة بين مفاصل الجسور والاعمدة الخرسانية بوجود المفاصل الانشائية وبعدها وجودها كذلك اجريت دراسة واسعة تضمنت كل مايتعلق بالعوامل المؤثرة بالمفصل الانشائي. هذه العوامل تتضمن المواقع المختلفة للمفصل الانشائي، الحمل المحوري للعمود، المقاومة الانضغاطية للخرسانة ضمن الصبة الثانية ومقدار الحديد المار من خلال المفصل. من خلال تطوير برنامج الحاسوب المكتوب اصلا من قبل الدكتور احسان الشعرباف (P3DNFEA) وهو برنامج لتحليل المسائل ثلاثية الابعاد تحليلا لخطيا بطريقة العناصر المحددة، لادخال تاثير المفصل الانشائي اعتمادا على حقيقة انتقال قوة القص خلال السطح القصي اما عن طريق تداخل حبيبات الركام البارزة من كل وجه او عن طريق تاثير التوتيد للحديد المار من خلال ذلك السطح وذلك باستخدام مويلات فرونتيدو وميلارد بالتتابع. وبعد تطوير البرنامج وجراء التحليل تم الاستنتاج بان المفصل الانشائي الموجود ضمن مفاصل الجسور والاعمدة الخرسانية يؤدي الى تناقص ملحوظ في الصلابة القصية وهو يؤثر فقط على دوران المفصل وعلى الانفعالات القصية فيه.

KEYWORDS

Beam-column junction, Reinforced concrete, Finite elements, Construction joints

INTRODUCTION

The junctions studied are made of two pours, this results in a cold joint. The existence of a cold joint means that the specimens simulate construction practice. In addition to the overall behaviour of the beam-column junction during each stage of loading, it is important to note the mode of failure in this region. Five different modes of failure are possible in the beam-column connection, these include the following:

- 1) Hinging of the beams at the connection, Fig.(1.a).
- 2) Hinging of the column, Fig.(1.b).
- 3) Loss of the concrete cover over the reinforcement in the beam-column core, Fig.(1.c).
- 4) The loss of anchorage of the reinforcement, Fig.(1.d).
- 5) The consequences of failure of the connection in shear, Fig.(1.e).

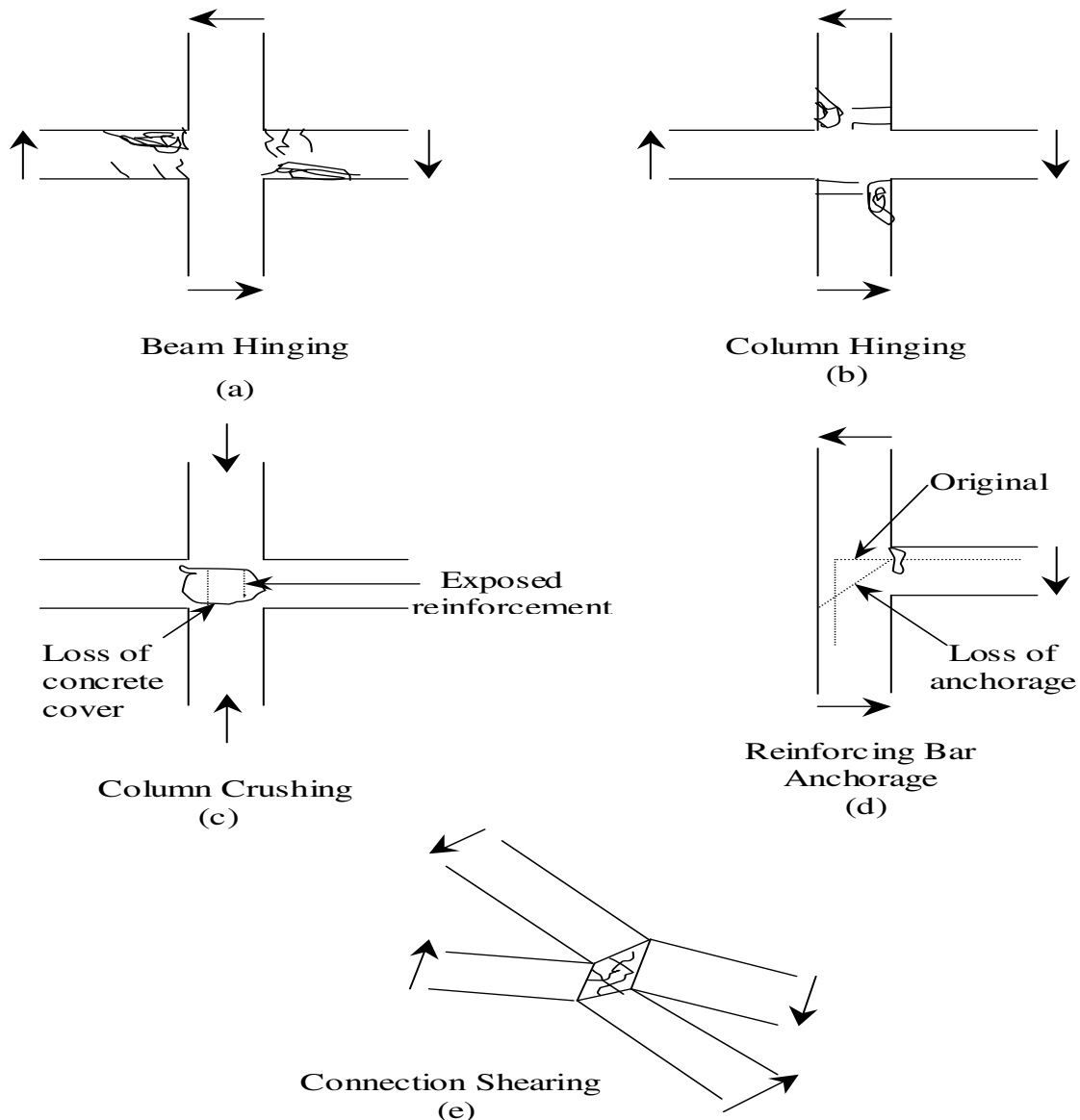


Fig.(1) Failure modes for beam-column connection
(Meinheit et al.(1981))



MATERIAL MODELLING

In addition to the original three-dimensional computational model of P3DNFEA, the models used in the present study and incorporated in the present developed program are as follows:

- 1) Theoretical Aggregate Interlock Models
- 2) Theoretical Dowel Action Models

ORIGINAL THREE-DIMENSIONAL COMPUTATIONAL MODEL

The 3-D computational model of original computer program, P3DNFEA is now described.

The behaviour of concrete is simulated by using 20-noded brick elements. An elasto-plastic work hardening model followed by a perfectly plastic response, which is terminated at the onset of crushing is adopted for concrete in compression. The plasticity model was illustrated in terms of the following constituents:

- 1) The yield criterion of two stress invariants (Cervenka (1985)).
- 2) An isotropic hardening rule is used (Cervenka (1985)).
- 3) An associated flow rule (Owen and Hinton (1980)).
- 4) The crushing rule.

In tension, a smeared crack model with fixed orthogonal cracks is used (Rashid (1968)). The reinforcing bars are idealized as axial members embedded within the brick elements, the elastic-perfectly plastic relation which ignores the strain-hardening region is used.

THEORETICAL AGGREGATE INTERLOCK MODELS

Several models have been proposed to explain or predict the aggregate interlock behaviour. The two-phase model by Walraven and Reinhardt (1981) is an example of a physical model. That type of model gives a better understanding of the mechanism involved at the crack interface. The Yoshikawa et al. (1989) model is an example of an empirical model, in which a free slippage occurs in the initial shear load on the cracked planes, which are not in close contact, and further application of the shear stress makes the cracks stiffer due to firm contact (aggregate interlock). Finally, the shear stress levels off approaching the ultimate shear strength. The Tassios and Vintzeleou (1987) model is another example of empirical model. It covers two types of interfaces, the rough interface and the smooth interface, for normal stresses ranging up to 2 MPa, in this model, the frictional resistance is roughly equal to the tensile strength of concrete, taking into account the tensile strength reduction due to a transverse compressive stress as follows:

$$\tau_u = (0.3 (10 + 9 (\sigma_c / f_t) - (\sigma_c / f_t)^2)^{0.5}) f_t \quad (1)$$

Fronteddu et al. (1998) utilized their experimental results from displacement controlled shear tests on concrete lift joint specimens with different surface preparations, to propose an empirical interface constitutive model based on the concept of basic friction coefficient (μ_b) and roughness friction coefficient (μ_i):

$$\mu = \frac{\lambda_d \mu_b + \chi_i \mu_i}{1 - \lambda_d \chi_i \mu_b \mu_i} \quad (2)$$

where $\mu_b = 0.950 - 0.220 \sigma_n$ for $\sigma_n \leq 0.5$ Mpa

$\mu_b = 0.865 - 0.050 \sigma_n$ for $0.5 \leq \sigma_n \leq 2.0$ Mpa

μ_i is defined by the equations in Table (1). Two correction factors were introduced: (1) λ_d , the dynamic reduction factor equal to 1.00 for static loading, and 0.85 for dynamic loading; and (2) χ_i , the interface roughness factor equal to 1.00 for cracked homogeneous concrete, 0.8 for water blasted joints, 0.15 for untreated joints, and 0.00 for flat independent concrete surfaces.

Based on the experimental results presented by Fronteddu et al. (1998), a bilinear relationship between shearing stress and slip, Fig. (2), is adopted, which is multiplied by the effective thickness of the Gaussian point of interface element to convert it to a relationship between shearing stress and strain. From Eqs.(1-2) a good prediction of aggregate interlock stiffness can be obtained.

Table (1) Concrete interface model roughness coefficient
(Fronteddu et al. (1998))

Interface type	σ_n (Mpa)	Peak μ_{ib}
Homogeneous	$\sigma_n \leq 0.4$	$0.90 - 1.367 \sigma_n$
	$0.4 \leq \sigma_n \leq 1.5$	$0.40 - 0.1167 \sigma_n$
	$1.5 \leq \sigma_n \leq 2$	$0.30 - 0.050 \sigma_n$
Water- blasted	$\sigma_n \leq 0.275$	$0.875 - 1.75 \sigma_n$
	$0.275 \leq \sigma_n \leq 1.2$	$0.44 - 0.185 \sigma_n$
	$1.2 \leq \sigma_n \leq 2$	$0.25 - 0.0375 \sigma_n$
Untreated	$\sigma_n \leq 1.0$	$0.15 - 0.15 \sigma_n$
	$1.0 \leq \sigma_n \leq 2.0$	$0.05 - 0.005 \sigma_n$

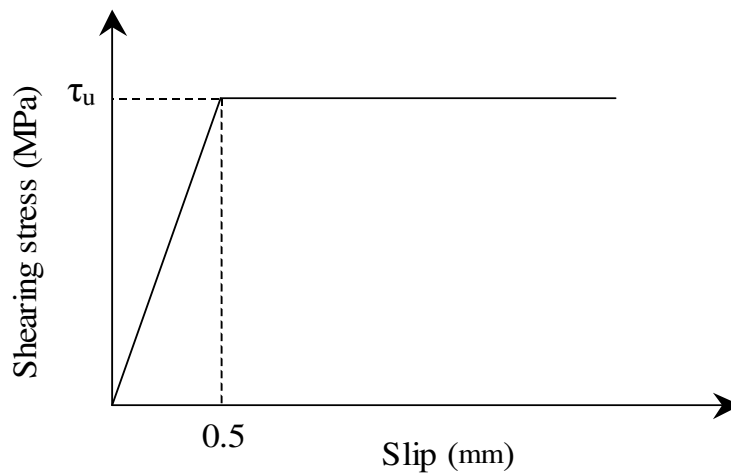


Fig. (2) Adopted shearing stress-slip relationship

THEORETICAL DOWEL ACTION MODELS

Shearing forces can be transmitted across a crack in the reinforced concrete by the reinforcement crossing the crack. If the reinforcement is normal to the plane of cracking, dowel action (shearing and flexure of the bars) will contribute to the overall shear stiffness.

It has been suggested (Paulay et al. (1974)) that there are three mechanisms of shear transfer through the dowel action in cracked reinforced concrete, i.e. direct shear, kinking and flexure of the bars. If the concrete supporting each bar were considered to be rigid, the first two mechanisms would predominate. However, it has been recognized (Mills (1975)) that significant deformation of the concrete does occur, so that flexure of the dowel bar within the concrete is a principal action. This has been modelled (Millard (1984)) by considering the dowel bar as a beam on elastic foundation. This model is adopted, according to this model the dowel force, F_d is given by:

$$F_d = 0.166 \Delta_t G_f^{0.75} \Phi^{1.75} E_s^{0.25} \quad (3)$$

where the constant term is dimensionless

G_f : foundation modulus for concrete, A typical value for 35 MPa concrete has been found to be 750 N/mm^3 (ACI Committee 325). For the high strength mix, it has been assumed that $G_f \propto f_{cu}^{0.5}$.

Φ : diameter of the bar.

E_s : elastic modulus of steel.

Δ_t : slip or relative displacement across the crack.

Only the initial dowel stiffness can be predicted using this equation.

The nonlinear shear stiffness of the dowel action may be attributed to one or both of the following two causes.

- 1) Crushing or splitting of the concrete supporting the bar.
- 2) Plastic yielding of the reinforcement.

A good prediction of the ultimate shearing force in a bar with an axial stress of αf_y is given by:

$$F_{du} = 1.3 \Phi^2 f_{cu}^{0.5} (f_y (1 - \alpha^2))^{0.5} \quad (4)$$

where F_{du} is the ultimate dowel force.

An exponential function was used to describe the overall dowel action behaviour. The dowel force, F_d , is as follows:

$$F_d = F_{du} (1 - \exp(-k_i \Delta_t / F_{du})) \quad (5)$$

where k_i is the initial dowel stiffness given by Eq.(3). By simplifying Eq.(5), the shear stiffness of the dowel action which is used in the present study as a relationship between the shearing stress and shear strain can be found as follows:

$$k_d = (k_i - \frac{k_i^2 \Delta_t}{2F_{du}}) t / A_c \quad (6)$$

where t is the effective thickness of the Gaussian point of the interface element (next section), A_c is the contact area.

FINITE ELEMENT IDEALIZATION OF INTERFACE REGION

An isoparametric finite element formulation, which is treated essentially like a solid element, can be used in the present study to represent the behaviour of the interface region (Desai and Zaman (1984)), Fig.(3). Since the element is treated essentially like any other solid element, its incremental stress-strain relationship is expressed as:

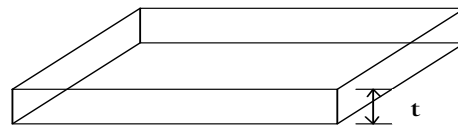
$$\{d\sigma\} = [D]_i \{d\varepsilon\} \quad (7)$$

where $[D]_i$ is the constitutive matrix for the interface region. The behaviour of the interface material is assumed to be like the concrete of the softer material properties for all stages of loading except the shear component which represents the shear behaviour specified for the interface region, (G_t , is the shear component represents the combination effects of aggregate interlock and dowel action), the constitutive matrix for the interface element can be written as:

$$[D]_i = \frac{E}{(1 + \nu)(1 - 2\nu)} \begin{bmatrix} 1-\nu & \nu & \nu & 0 & 0 & 0 \\ \nu & 1-\nu & \nu & 0 & 0 & 0 \\ \nu & \nu & 1-\nu & 0 & 0 & 0 \\ 0 & 0 & 0 & G_t & 0 & 0 \\ 0 & 0 & 0 & 0 & G_t & 0 \\ 0 & 0 & 0 & 0 & 0 & G_t \end{bmatrix} \quad (8)$$

The interface behaviour depends on the properties of the surrounding media. However, it also depends on the thickness of the thin-layer element. If the thickness is too large in comparison with the average contact dimension (B), of the surrounding element, the thin-layer element will behave essentially as a solid element. On the other hand, if it is too small, computational difficulties may arise. Based on the available experimental results, the satisfactory simulation of the interface behaviour can be obtained for (t / B) ratios in the range from (0.01) to (0.1). This conclusion may need modification if the nonlinear behaviour of solids and interfaces were simulated. The 20-noded isoparametric brick element is used.

SARSAM'S SPECIMENS



Nine specimens of beam-column joints (5 exterior, and 4 interior) were tested by Sarsam (1983), the plane exterior ones-EX series. Fig.(3) Thin layer interface element made on the first day. This pour included the specimen up to the level of the top of the joint. The second pour was made on the next day for the top column.

All columns were reinforced with four 16mm longitudinal bars and 8mm closed links at 85mm center to center spacing, giving three joint links. Only specimen EX2 has no links in the joint. All beams were reinforced with two 16mm bars on the tension side and two 12mm bars on the compression side. Beam links were 8mm closed ones spaced at 130mm center to center.

The EX1, EX3 specimens are used in the present study, of dimensions shown in Table(2), Fig.(4). Material properties and additional material parameters of these specimens are shown in Tables (3), (4), respectively. The column was first loaded to a predetermined value of (Nc), prior to any beam loading, the next stage involved loading the beam up to ultimate load. The numerical analysis is done using KT2a method, with a tolerance of 5% on the displacement convergence criterion.

Table (2) Dimensions of Sarsam’s specimens

Dimensions/ Specimens	Beam		Column		Lc (mm)	av (mm)	Column Load (kN)
	h (mm)	b (mm)	h (mm)	b (mm)			
Specimen EX1	303	152	205	152	1531	1422	292.6
Specimen EX3	305	152	204	152	1532	661	293.7

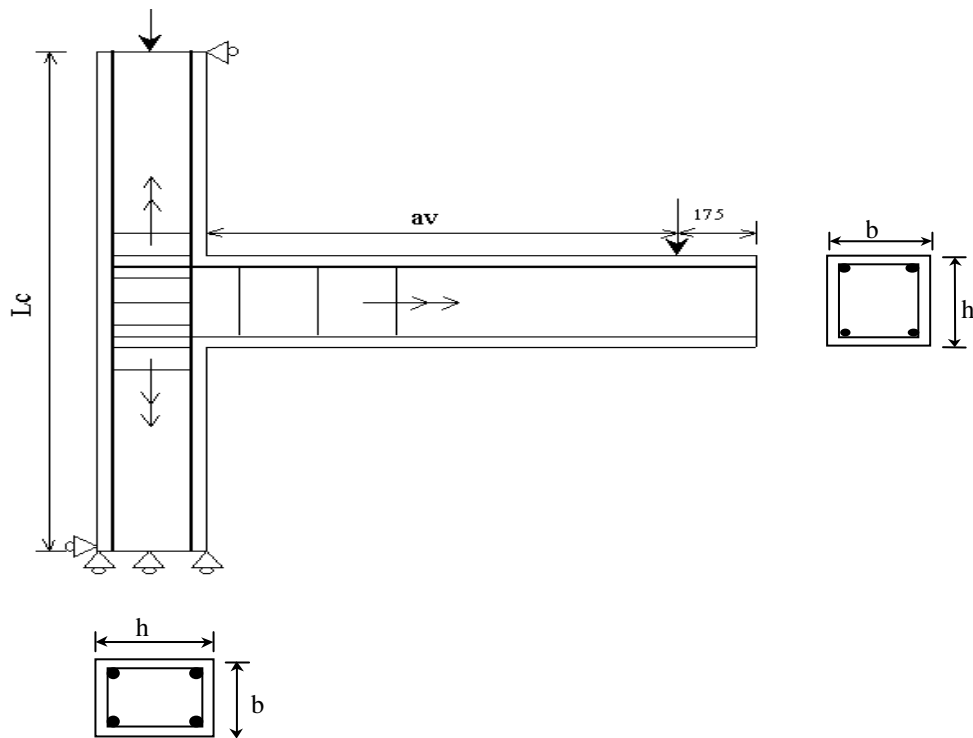


Fig.(4) Experimental corner beam-column joint specimen (Sarsam (1983))

Table (3) Material properties and additional material parameters of Sarsam’s specimen EX1

First pour (age=64 days)		
Material properties		Material parameters
Modulus of elasticity , E (MPa)	35500	Tension-stiffening parameters : $\alpha 1=35$, $\alpha 2=0.35$
Compressive strength, f'_c (MPa)	56.3	
Tensile strength , f_t (MPa)	4.5	Shear-retention parameters : $\gamma 1=25, \gamma 2=0.5, \gamma 3=0.1$
Poisson’s ratio , ν	0.2*	
Uniaxial crushing strain	0.00238	



Second pour (age=63 days)				
Material properties			Material parameters	
Modulus of elasticity , E (MPa)	30600		Tension-stiffening parameters : $\alpha 1=25$, $\alpha 2=0.25$ Shear-retention parameters : $\gamma 1=25, \gamma 2=0.5, \gamma 3=0.1$	
Compressive strength, f'_c (MPa)	45.8			
Tensile strength , f_t (MPa)	3.93			
Poisson's ratio , ν	0.2*			
Uniaxial crushing strain	0.003*			
Steel reinforcement				
Longitudinal bar $\Phi 16$	Young's modulus (MPa)	208000	Yield stress (MPa)	504
Longitudinal bar $\Phi 12$		198000		507
Stirrup bar $\Phi 8$		197000		517

Table (4) Material properties and additional material parameters of Sarsam's specimen EX3

First pour (age=39 days)				
Material properties			Material parameters	
Modulus of elasticity , E (MPa)	28000		Tension-stiffening parameters : $\alpha 1=20$, $\alpha 2=0.20$ Shear-retention parameters : $\gamma 1=25, \gamma 2=0.5, \gamma 3=0.1$	
Compressive strength, f'_c (MPa)	41.3			
Tensile strength , f_t (MPa)	3.44			
Poisson's ratio , ν	0.2*			
Uniaxial crushing strain	0.00701			
Second pour (age=38 days)				
Material properties			Material parameters	
Modulus of elasticity , E (MPa)	28200		Tension-stiffening parameters : $\alpha 1=19$, $\alpha 2=0.19$ Shear-retention parameters : $\gamma 1=25, \gamma 2=0.5, \gamma 3=0.1$	
Compressive strength, f'_c (MPa)	40.9			
Tensile strength , f_t (MPa)	3.56			
Poisson's ratio , ν	0.2*			
Uniaxial crushing strain	0.003*			
Steel reinforcement				
Longitudinal bar $\Phi 16$	Young's modulus (MPa)	208000	Yield stress (MPa)	504
Longitudinal bar $\Phi 12$		198000		507
Stirrup bar $\Phi 8$		197000		517

1) Finite Element Description

The concrete of specimens EX1 and EX3 are idealized by using 58 20-noded brick elements (including 1 interface element at the top level of the joint), and 37 20-noded brick elements (including 1 interface element at the top level of the joint), respectively (for half of these specimens), Fig.(5). To simulate the procedure of loading that occurred during the experimental test, the column axial load has been firstly applied in equal increments of 10% of the maximum column load for two specimens. Later, for EX1 two different sizes of increments have been used for beam loading. The beam was loaded initially by increments of 3.75kN up to 75% of the expected collapse load (40kN). Then reduced increments of 1.43kN each were applied until the failure load has been reached. While for EX3 the beam load has been applied in equal increments of 12.5% of the expected collapse load (80 kN). Both the initial and post-cracking stiffness are reasonably predicted for two specimens, Table (3), Table (4).

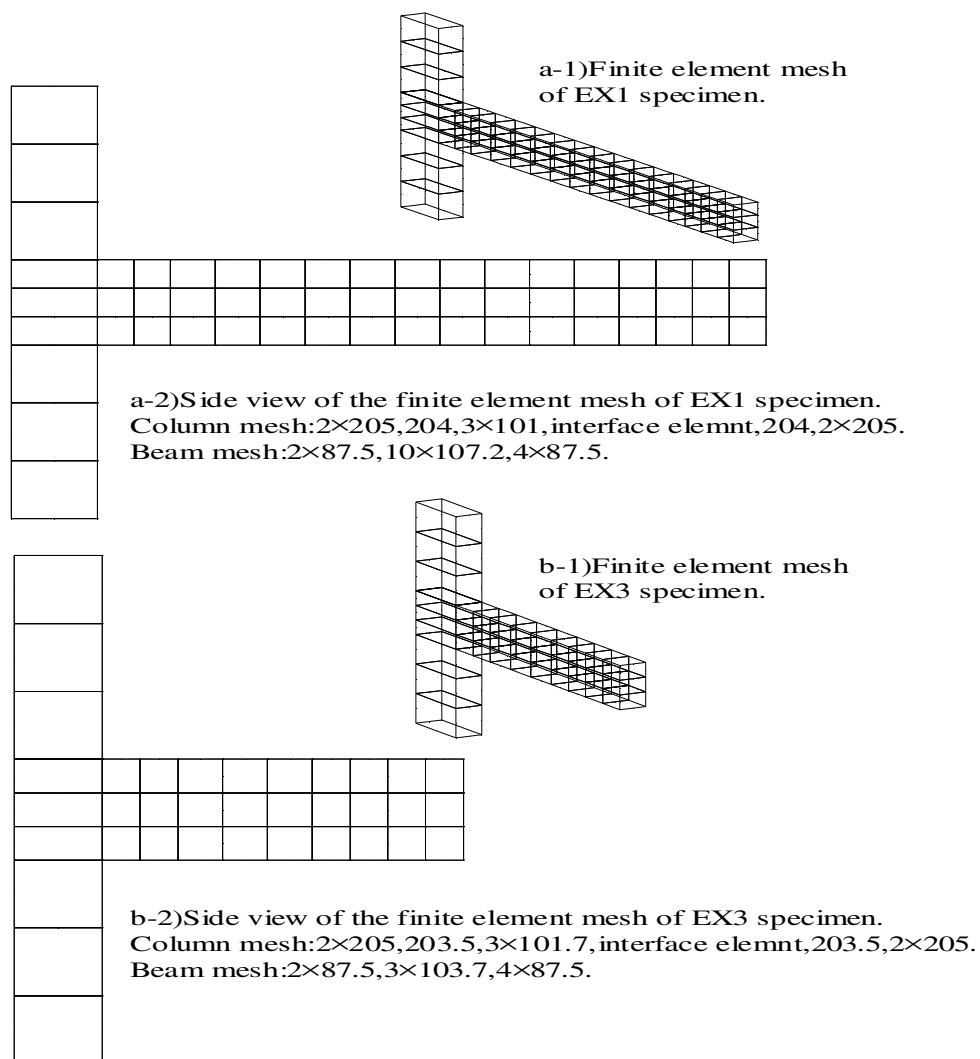


Fig.(5) Finite element discretization of half of EX1, and EX3 specimens.

Analysis of the Specimens

In order to analyze the two specimens, the effect of the thickness of interface element must be examined. For EX1 specimen, numerical tests with values of the thickness (t) equal to 0.014mm, 0.14mm, and 1.4mm have been carried out. The results show that the type of failure of the specimen EX1 is beam hinging in the range of (0.014-0.14)mm for thickness of interface element, Fig.(6). A response stiffer than the experimental results was obtained when the thickness is reduced within the range, and the best fit to the experimental results was obtained at $t=0.14$ mm with effective thickness of Gaussian point of 0.038mm, in which the effect of non-linearities along the loading stages is clear. The failure load of numerical results is 37.5kN while the failure load of experimental results is 36.04kN, so that the error ratio is 3.9%. While for EX3 specimen, numerical tests with values of the thickness (t) equal to 0.0014mm, 0.014mm, and 0.14mm have been carried out. The results show that the type of failure of the specimen EX3 is beam hinging in the range of (0.0014-0.014)mm for thickness of interface element, Fig.(7). A stiffer response was obtained when the thickness is reduced, and the best fit to the experimental results was obtained at $t=0.0014$ mm with effective thickness of Gaussian point of 0.00038mm. The failure load of numerical results is 80kN while the failure load of experimental results is 78.7kN, so that the error ratio is 1.6%. In the present study the value of thickness of the interface element equal to 0.14mm is fixed for EX1 specimen to present a parametric study.

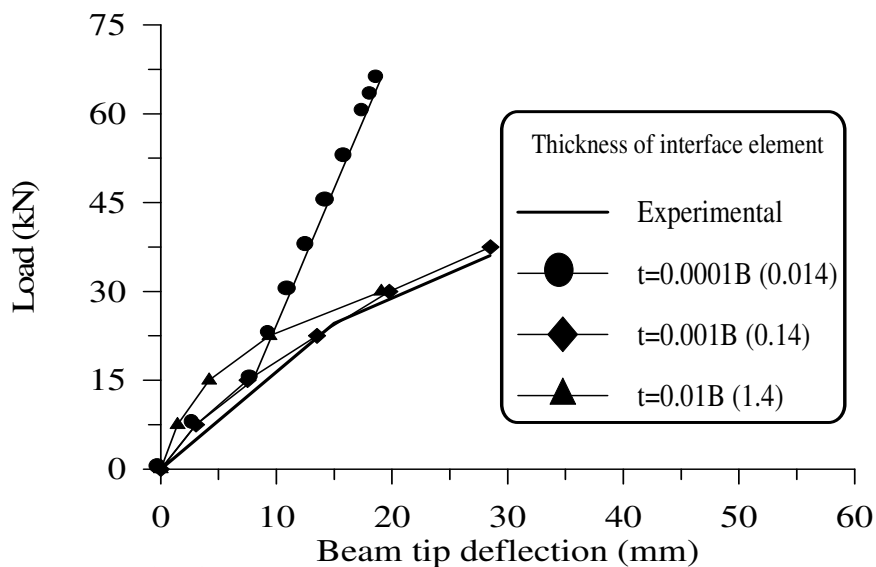


Fig.(6) Comparison between experimental and analytical response of different interface thickness values for EX1

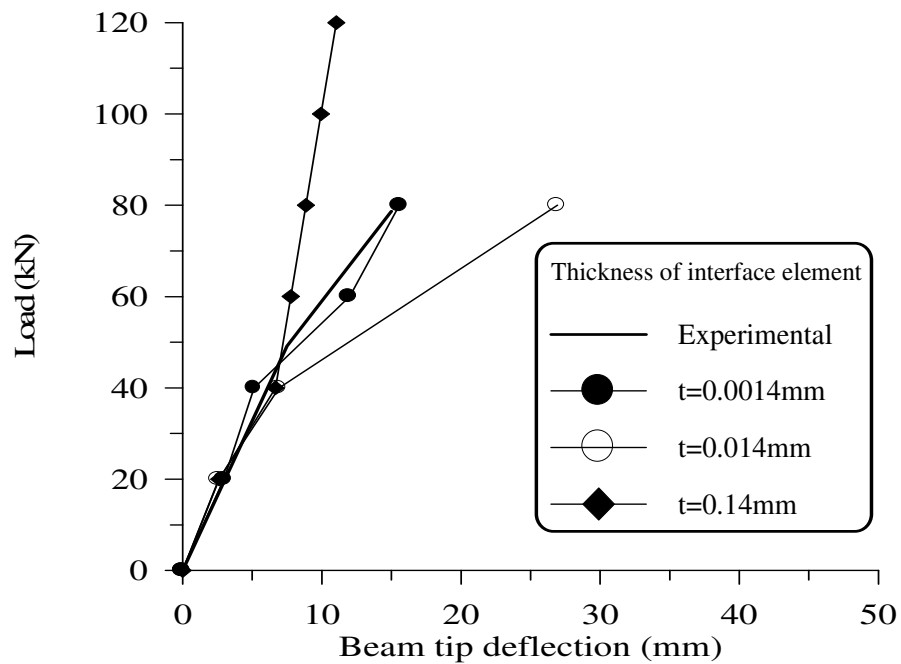


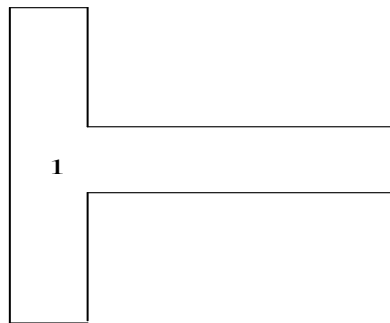
Fig.(7) Comparison between experimental and analytical response of different thickness value for EX3 specimen.

PARAMETRIC STUDY

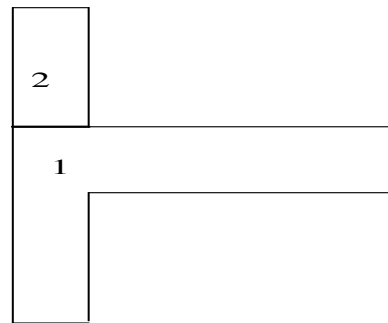
A parametric study deals with construction joint is presented by taking various conditions of the junction. These include the various positions of the construction joint, the axial load on the column, strength of concrete in the second cast and the amount of dowels crossing the joint as follows:

THE EFFECT OF POSITION OF CONSTRUCTION JOINT

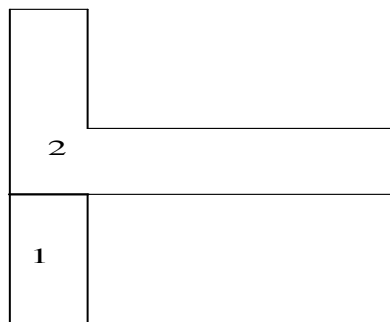
In order to study the effect of the position of construction joint (c.j.), a numerical study on four cases have been carried out, Fig.(8), case (a) without c.j., case (b) with c.j. at the top level of the joint, case (c) with c.j. at the bottom level of the joint, and case (d) with 2 c.j. one at the top level and the other at the bottom level of the joint. These cases were made of three pours (1,2,3) of material properties shown in Table (5). Fig.(9) represents load-tip deflection of these cases. As a result of comparison between curves, a soft response occurred for cases with c.j., the response of case (c) is softer than the response of case (b), and a softer response of all is observed for case (d). It is worth noting that the mode of failure in all cases is beam hinging.



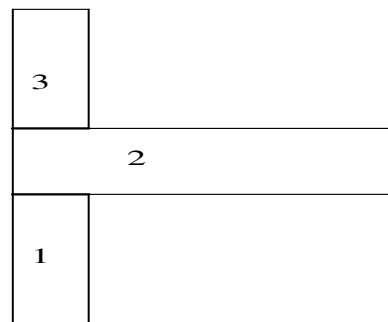
Case (a) Monolithic specimen (without construction joint)



Case (b) Composite specimen (with construction joint at top level of joint)



Case (c) Composite specimen (with construction joint at bottom level of joint)



Case (d) Composite specimen (with 2 construction joint at top & bottom levels of joint)

Fig (8) Cases of construction joints of beam-column joint

Table (5) Material properties and additional material parameters of Sarsam's specimen EX1

First pour (1) (age =64 days)		
Material properties		Material parameters
Modulus of elasticity , E (MPa)	35500	Tension-stiffening parameters : $\alpha 1=35 , \alpha 2=0.35$ Shear-retention parameters: $\gamma 1=25, \gamma 2=0.5, \gamma 3=0.1$
Compressive strength, f'_c (MPa)	56.3	
Tensile strength , f_t (MPa)	4.5	
Poisson's ratio , ν	0.2*	
Uniaxial crushing strain	0.00238	
Second pour (2) (age =63 days)		
Material properties		Material parameters
Modulus of elasticity , E (MPa)	30600	Tension-stiffening parameters : $\alpha 1=25 , \alpha 2=0.25$ Shear-retention parameters: $\gamma 1=25, \gamma 2=0.5, \gamma 3=0.1$
Compressive strength, f'_c (MPa)	45.8	
Tensile strength , f_t (MPa)	3.93	
Poisson's ratio , ν	0.2*	
Uniaxial crushing strain	0.003*	
Third pour (3) (age =62 days)		
Material properties		Material parameters

Modulus of elasticity , E (MPa)	29200	Tension-stiffening parameters : $\alpha 1=25$, $\alpha 2=0.25$ Shear-retention parameters: $\gamma 1=25, \gamma 2=0.5, \gamma 3=0.1$
Compressive strength, f'_c (MPa)	43.3	
Tensile strength , f_t (MPa)	3.31	
Poisson's ratio , ν	0.2*	
Uniaxial crushing strain	0.003*	

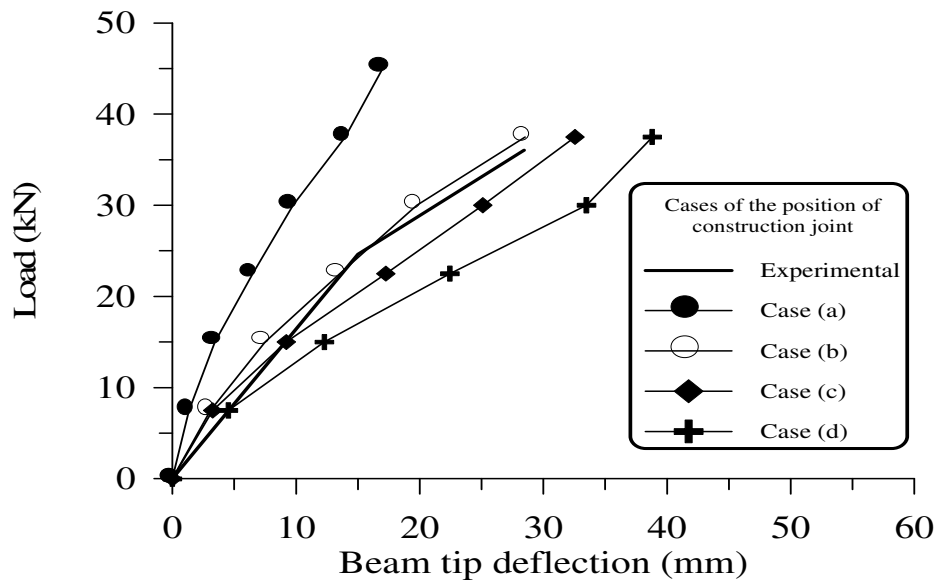


Fig.(9) Load-beam tip deflection for cases of construction joints.

THE EFFECT OF CONSTRUCTION JOINT

There are different contributions to beam tip deflection. The first one is the contribution of joint shear strain, the second involves the contribution of joint rotation, and the third is the contribution of beam flexure. To examine the effect of the construction joint on the behaviour of the specimen, the shear, and normal strains in the joint (at 63.4mm left to the column face), and the normal strains in the beam (at 77.65mm right to the column face) are studied for case b (construction joint at the top level of the joint) and compared with strains of the monolithic specimen (case a) as follows:

From Fig (10), and Fig.(11), the shear and normal strains in the joint for case (b) are greater than the strains for case (a) (monolithic). The amount of increment of strains near the construction joint is larger than the strains in other positions of joint. These results refer to the occurrence of several short diagonal tension cracks along the length of the shear plane (construction joint), and these cracks cause a reduction in shear and in normal stiffness. While the normal strains in beam, Fig.(12), are not much affected by the construction joint. This means that the construction joint affect only on the behaviour of the joint itself.

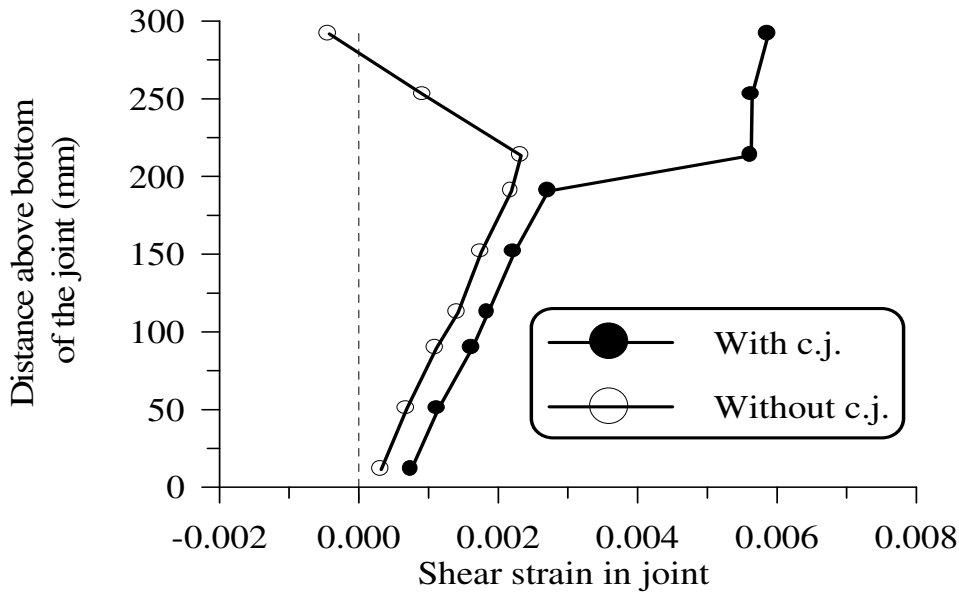


Fig.(10) Shear strains distribution in joint for case a (monolithic) and case b (construction joint at the top level of joint)

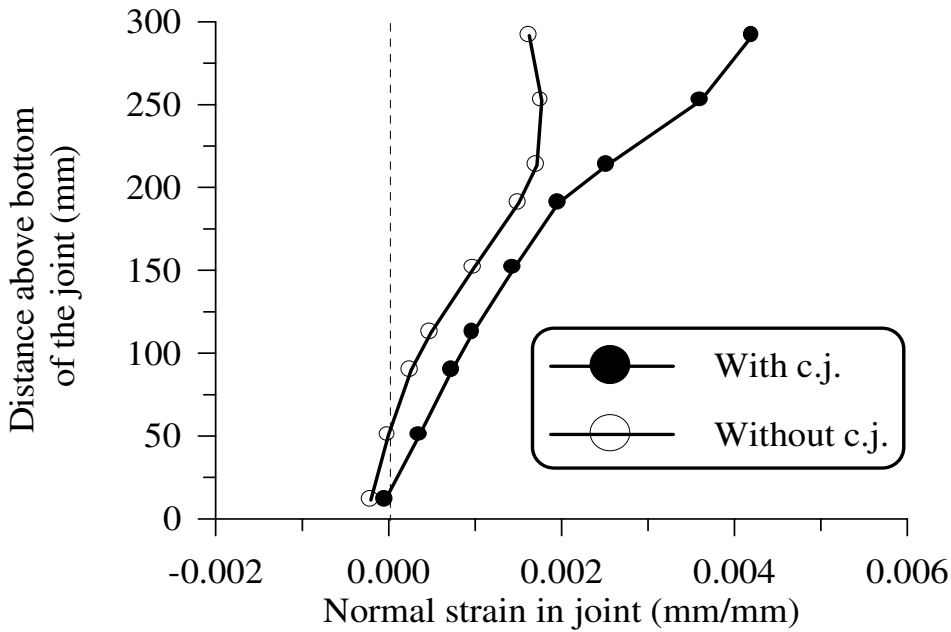


Fig.(11) Normal strains distribution in joint for case a (monolithic) and case b (construction joint at the top level of joint)

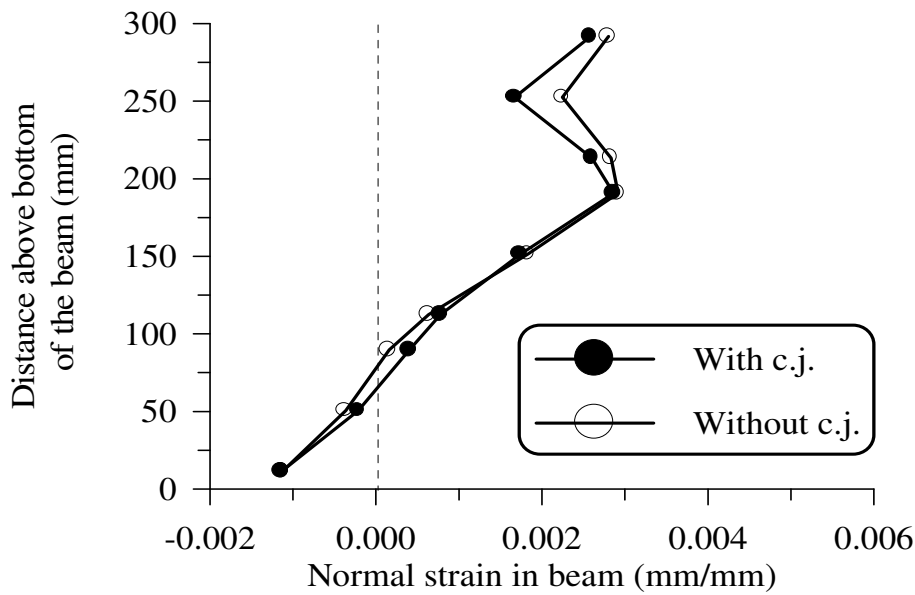


Fig.(12) Normal strains distribution in beam for case a(monolithic) and case b (construction joint at the top level of

The Effect of Column Axial Load

In order to expect the effect of column axial load on the behaviour of construction joint, a numerical study have been carried out, one with experimental column axial load ($N_c=292.6\text{kN}$), and the other without column axial load ($N_c=0.0$) for case (b) (construction joint at the top level of the joint). It can be observed from Figs.(13) and (14) that the shear and normal strains in the joint for $N_c=0.0$ are less than the strains for $N_c=292.6\text{kN}$. A possible explanation of this feature may be the following: Higher compressive stresses (at $N_c=292.6\text{kN}$), in spite of the more intimate interlocking they secure, produce a shortening of the protruding asperities and subsequently reduce overriding resistance. This mechanism does not happen at $N_c=0.0$. On the contrary, due to loss of the confinement for $N_c=0.0$, the response of the specimen is softer than the response for $N_c=292.6\text{kN}$, Fig.(15) .

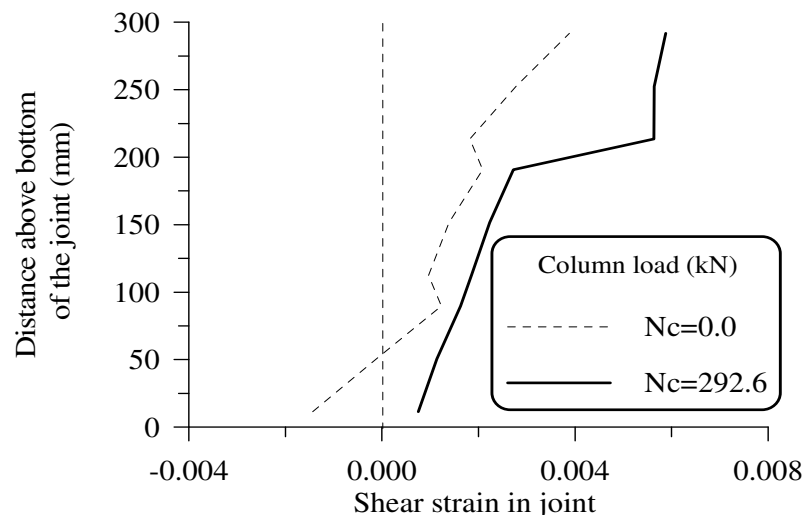


Fig.(13) Shear strains distribution in joint for case b (construction joint at the top level of joint)

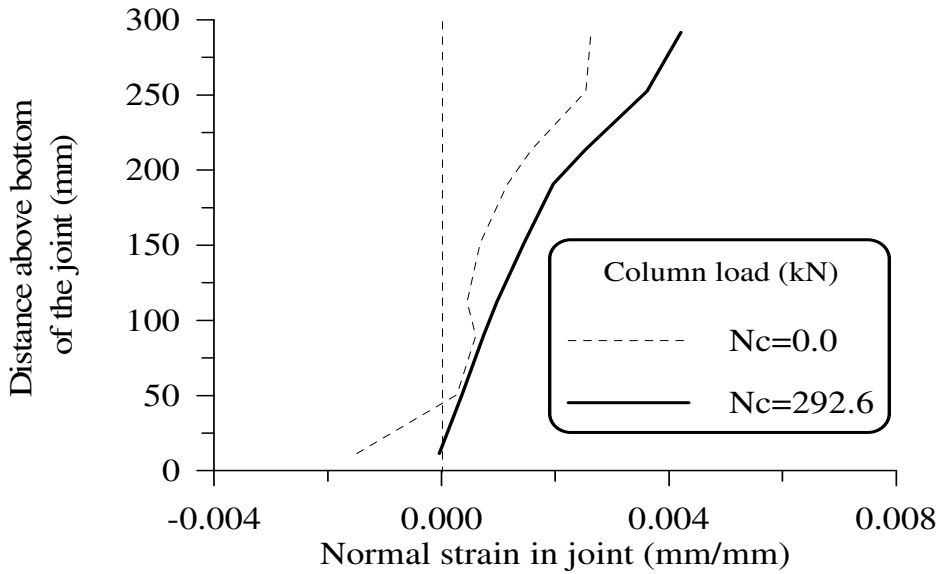


Fig.(14) Normal strains distribution in joint for case b (construction joint at the top level of joint)

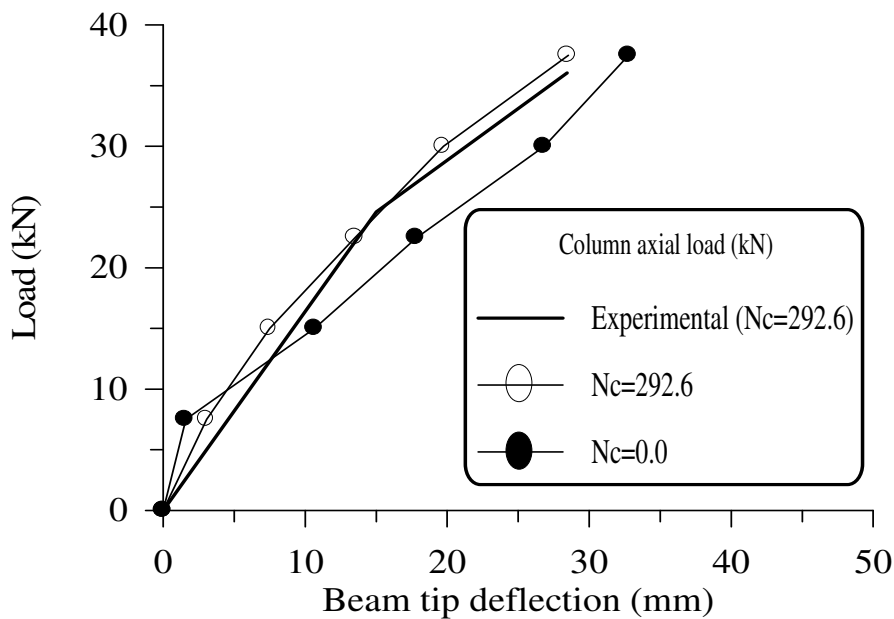


Fig.(15) Load- beam tip deflection for case b (construction joint at the top level of joint)

THE EFFECT OF THE AGE OF CONCRETE

The age of concrete pour has an effect on the compressive strength of the concrete. In order to study the effect this age, three tests have been carried out with f_c values equal to 45.8, 40, 30 MPa, Fig.(16). These values of strengths are for ages approximately equal to 63, 38, 20 days, respectively for the second pour of case (b), including the construction joint. These tests show that the higher concrete compressive strength results in a slight increase in aggregate interlock stiffness of construction joint.

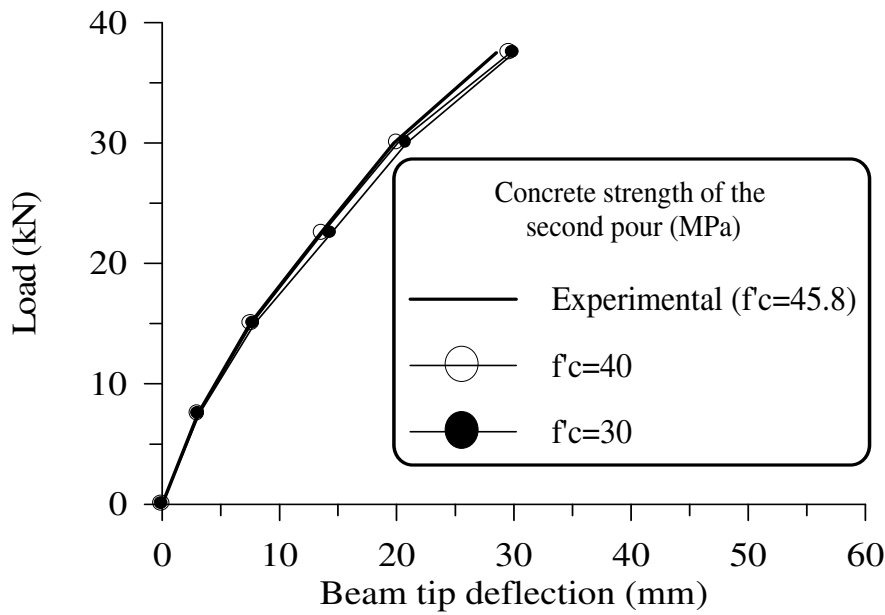


Fig.(16). Effect of compressive strength of concrete on the load-beam tip deflection curve for case b (construction joint at the top level of joint)

The Effect of the Percentage Steel Across the Construction Joint

Three numerical tests have been carried out by using the percentage steel across the construction joint (diameter of the bar) of 0.031 (16mm), 0.033 (18mm), and 0.048 (20mm) for case (b), construction joint at the top level of joint, these tests occurred with original designed specimen. From Fig.(17) that the deflection decrease with the increase in the steel percentage across the construction joint (column reinforcement), the contribution in this result is the decreased strains in joint due to increase in dowel stiffness.

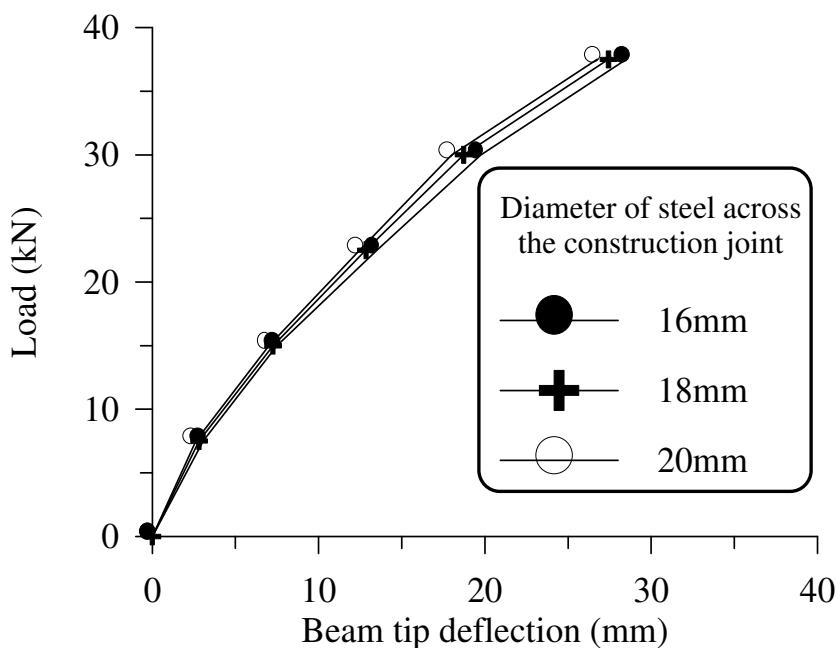


Fig.(17) Effect of diameter of crossed steel on the load-beam tip deflection curve for case b (construction joint at the top level of joint)



CONCLUSIONS

The following conclusions can be drawn from the present study:

1. A good assessment can be obtained for the behaviour of corner beam-column joints by using the developed program of the current study (DPACJ).
2. The performance of the interface element , used in this study to model the shear transfer between two concretes cast in different times, is quite good.
3. A stiff response can be obtained with the decrease in the thickness of the interface element.
 4. The response of a specimen can be expected within a certain range of thickness of interface element. This range depend on the finite element mesh, nonlinear behaviour of material, and the combination of stresses.
 5. Construction joint is a joint of weakness. Depending on the position of construction joint, the shear and normal strains in joint would increase.
 6. The construction joint would affect only on the joint. On the other hand, the mode of failure for all cases of corner beam-column joint in this study is beam hinging, this type of failure conforms with the design requirements.
7. The presence of column axial load would decrease the aggregate interlock stiffness. However, it secures a good confinement for the beam, and so as the result of increase it.
 8. The grade of concrete of the second pour, producing a construction joint, does not much affect the behaviour of the corner beam-column joint.
 9. The increase of steel percentage across the construction joint would decrease the strains in joint. Consequently, a slightly decrease of deflection occurred.

REFERENCES

ACI Committee 318,(1995).“Building Code Requirements for Reinforced Concrete (ACI 318-95).” American Concrete Institute, Detroit.

ACI Committee 325, (1956) (Cairman: FINNEY. E.) Structural Design Considerations for Pavement Joints. J. Ame. Con. Inst. Proce., 53(1), July, 1-28, (Cited according to Millard and Johnson (1984)).

Al-Shaarbaf I.(1990).“Nonlinear Three Dimensional Finite Element Analysis Program for Steel and Reinforced Concrete Beam in Torsion.” Ph.D. Thesis, University of Bradford.

Cervenka V.(1985).“Constitutive Model for Cracked Reinforced Concrete.” ACI J.,82(6),877-882,November-December.

Desai C.S., Zaman M.M.,Lightner J.G.,and Siriwardane H.J.(1984).“Thin-Layer Element for Interfaces and Joints.”J. Nume. Analy. Meth. Geome.,8,19-43.

Fronteddo L.,Léger P.,and Tinawi R.(1998).“Static and Dynamic Behaviour of Concrete Lift Joint Interfaces.”J. Struct. Engrg.,ASCE,124(12),1418-1430.

Meinheit D.F.,Jirsa J.O., and Members of ASCE(1981).“Shear Strength of Reinforced Concrete Beam-Column Connections.”ASCE,107(ST11).

Mills G.M.(1975).“A Partial Kinking Criterion for einforced Concrete Slabs.” Maga. Conc. Resea.,27(90),13-22.

Millard S.G.,and Johnson R.P.(1984).“Shear Transfer across Cracks in Reinforced oncrete due to Aggregate Interlock and to Dowel Action.” Maga. Conc. Resea.,36(126).

Owen D.R.,and Hinton E.(1980).“Finite Element in Plasticity, Theory and Practice. ”Pineridge Press, Swansea,U.K.

Paulay T.,and Loeber P.J.(1974).“Shear Transfer by Aggregate Interlock. ”Shear in Reinforced Concrete, Detroit, American Concrete Institute,ACI Special Publication SP 42-1.1,1-15,(Cited according to Millard and Johnson (1984)).

Rashid Y.R.(1968).“Analysis of Prestressed Concrete Pressure Vessels. ”Nucl. Engng. Desi.,7(4).

Sarsam K.F.(1983).“Strength and Deformation of Structural Concrete Joints. ”Ph.D. Thesis, University of Manchester.

Tassios T.P.,and Vintzèleou E.N.(1987).“Concrete-to-Concrete Friction. ”J. Struc. Engrg., ASCE, 114(9), 2133-2136.

Walraven J.C.,and Reinhardt H.W.(1981).“Concrete Mechanics, Part A. Theory and Experiments on the Mechanical Behaviour of Cracks in Plain and Reinforced Concrete Subjected to Shear Loading. ”Heron.26(1A),1-68, (Cited according to Millard and Johnson (1984)).